Grid-Edge Real-Time Abnormal Event Detection in Point-on-Wave Data with Lightweight Matrix Profile

Koji Yamashita and Nanpeng Yu
Electrical and Computer Engineering
University of California, Riverside
Riverside, CA, USA
kyamashi@ucr.edu, nyu@ece.ucr.edu

Bo Chen and Ruoxi Zhu
Smart Grid Emerging Technology
Commonwealth Edison Company
Chicago, IL, USA
bo.chen@comed.com, ruoxi.zhu@comed.com

Neeraj Nayak
Advanced Applications and Analytics
Electric Power Group
Pasadena, CA, USA
nayak@electricpowergroup.com

***Abstract*—Point-on-wave (PoW) sensors provide high-resolution measurements for power grid monitoring, but their extremely high sampling rates pose major challenges for real-time processing due to communication bandwidth and computational resource constraints. This creates a need for computationally and memory-efficient algorithms suitable for grid-edge deployment. This paper proposes a lightweight Matrix Profile–based framework for real-time abnormal event detection using PoW measurements. The proposed method identifies informative electrical quantities for event detection by leveraging historical PoW data and labeled event records. To enhance robustness under severely unbalanced three-phase current conditions, washout filters and an adaptive time-varying thresholding scheme are introduced. The proposed approach is validated using more than one hundred real-world PoW measurement records. Experimental results demonstrate that the proposed method achieves reliable real-time event detection for PoW data sampled at 7,680 Hz while requiring only 5 MB of memory, making it well suited for deployment on resource-constrained grid-edge monitoring devices.**

***Index Terms*—Grid-Edge Monitoring, Matrix Profile, Point-on-Wave Measurements, Real-time Event Detection.**

I. Introduction

Phasor measurement units (PMUs) have been introduced into power system monitoring in the aftermath of the 2003 North American blackout, which exposed critical limitations in grid situational awareness and catalyzed the development of wide-area measurement systems. Since then, PMU-based monitoring systems have become a cornerstone of modern power system operation, providing time-synchronized measurements typically sampled at 30–60 Hz [1]. These measurements have proven highly effective for observing electromechanical dynamics and slow-to-medium timescale disturbances. However, the inherent limitation of the sampling rate constrains PMUs' capability to fully capture fast transient and switching phenomena, as well as certain converter-driven oscillations and high-frequency control interactions that are becoming more prevalent in modern power grids. Consequently, important high-frequency dynamic behaviors may be observed only partially or entirely missed, thereby limiting the performance of event detection and diagnosis in modern power systems.

Point-on-Wave (PoW) technology has recently emerged as a compelling complement to PMU-based monitoring by enabling high-bandwidth measurements directly from distribution grids. By providing substantially higher temporal resolution, PoW data offers enhanced visibility into fast system dynamics, including switching events, transient disturbances, and higher-frequency oscillatory behaviors. This improved observability creates new opportunities for early event detection, more precise disturbance characterization, and improved operational awareness. At the same time, the massive volume and speed of PoW data introduce significant challenges for real-time analytics, necessitating lightweight algorithms that can operate reliably at the grid edge with minimal model assumptions and limited processing resources.

Existing event detection techniques can be broadly categorized into statistical and signal processing–based approaches [2]–[7] and machine learning-based approaches [8]–[12]. The former exploit explicit statistical assumptions or signal structures, such as stochastic process models, low-rank subspace representations, and parametric filtering frameworks, to characterize nominal behavior and identify deviations as anomalies. Representative examples include Bayesian changepoint detection for PMU data streams [2], random matrix theory combined with Kalman filtering for robust event detection in both simulated and real-world systems [4], structured workflows for event classification from imperfect data [3], and singular value decomposition-based methods that capture low-dimensional structures and spatial correlations in synchrophasor measurements [5]. In practice, however, their performance is often sensitive to parameter drift, and the growing complexity of modern power systems, which limits their robustness in operational environments.

Machine learning-based approaches including supervised, weakly supervised, and unsupervised frameworks have been applied to large-scale PMU and micro-PMU datasets for event detection and classification, with validation on real-world utility data and near–real-time operation [8]. For example, weakly supervised learning has been used to reduce reliance on costly labeled data [11], while generative adversarial networks (GANs) and bidirectional GANs (BiGANs)-based methods have been proposed to capture complex spatio-temporal dependencies, enabling accurate detection of subtle or previously unseen events without requiring event labels [9], [10]. Despite these advances, many existing methods focus primarily on detection rather than systematic event discovery and labeling, which limits their usefulness for large-scale monitoring, post-event analysis, and knowledge base construction.

While extensive research has explored event detection and classification using PMU and micro-PMU measurements, relatively few studies have investigated event or anomaly discovery using high–temporal–resolution PoW or continuous PoW data [13]. Existing work on synchronized waveform measurements has primarily focused on foundational data representations, statistical inference frameworks, protection applications, and streaming data compression, rather than on systematic and lightweight event discovery pipelines. Although these studies highlight the strong potential of waveform-level sensing for enhanced visibility into fast grid dynamics beyond the capability of traditional phasors, dedicated PoW-based event discovery methodologies that are rigorously validated on realistic datasets remain scarce in the peer-reviewed literature, leaving a clear gap between high-bandwidth sensing capabilities and practical, deployable event analytics.

This paper presents a matrix profile (MP)–based framework for event detection using high-resolution PoW measurements, adapted for memory- and computation-efficient real-time operation on grid-edge monitoring devices. The MP is a model-free, unsupervised time-series technique that quantifies similarity between subsequences via nearest-neighbor distances, enabling robust anomaly detection — particularly for power quality events — without labeled data or prior system models. Existing MP algorithms are typically designed for offline or cloud-based processing with ample computational resources. The proposed enhancements extend the MP framework to streaming PoW data in resource-constrained environments, enabling reliable detection of fast transient events and decayed oscillatory behaviors directly at the data source, without reliance on centralized processing.

The remainder of this paper is organized as follows. Section II introduces the proposed streaming event discovery framework based on the MP values. Section III details the technical methodology. Section IV presents case studies with actual PoW data to evaluate the performance of the proposed lightweight MP-based power grid event detection algorithm.

II. Overview of Event Detection Framework

This paper presents an event detection method designed for streaming PoW data such that the detection process is completed before new samples arrive. Figure 1 illustrates the overall processing flow of the proposed framework, which consists of three stages. To ensure real-time applicability on resource-constrained platforms, both the number of required measurement channels and the data window length are minimized, enabling deployment on edge devices with limited computing power and memory.

In the first stage, the proposed framework utilizes the MP computed from three-phase current, zero-sequence voltage, and zero-sequence current signals. The MP values associated with each electrical signal are first computed then fused into a single composite MP metric using an L_2 norm-based integration, providing a compact indicator for event detection.

Under steady-state operating conditions, the MP values remain close to zero because the waveform exhibits highly periodic sinusoidal patterns. When an abnormal event occurs, the MP value increases sharply, resembling a step change, which enables effective detection using threshold-based logic. In practice, however, waveform distortions—particularly those arising from unbalanced loading and low-voltage operating conditions—can introduce bias into MP values. In the second stage, a washout filter is proposed to correct the bias.

Even with bias correction, high-amplitude oscillations in MP values may still produce false positive detections. In the third stage, an adaptive threshold scaling mechanism is introduced to enhance detection robustness. In this stage, recent MP statistics are used to dynamically adjust a nominal detection threshold. This strategy helps suppress false positive detections while preserving sensitivity to legitimate disturbance events.

Scalable Time series Anytime MP (STAMP) is an efficient MP calculation algorithm [14]. Mueen's Ultra-fast Algorithm for Similarity Search (MASS) is the core procedure in STAMP and accounts for most of its computational cost, as it computes the distance profile for each subsequence. In MASS, FFTW [15] is leveraged to accelerate the FFT operations. We integrate a lightweight FFTW-based implementation into the proposed framework, enabling real-time operation under practical deployment constraints.

III. Technical Method

A. Matrix Profile Formulation

Let $\mathbf{X} \in \mathbb{R}^{T \times D}$ denote a multivariate time series composed of three-phase voltage and current measurements together with their corresponding zero-sequence quantities, where D is the total number of channels and T is the length of the time series. The signal is uniformly sampled and segmented into

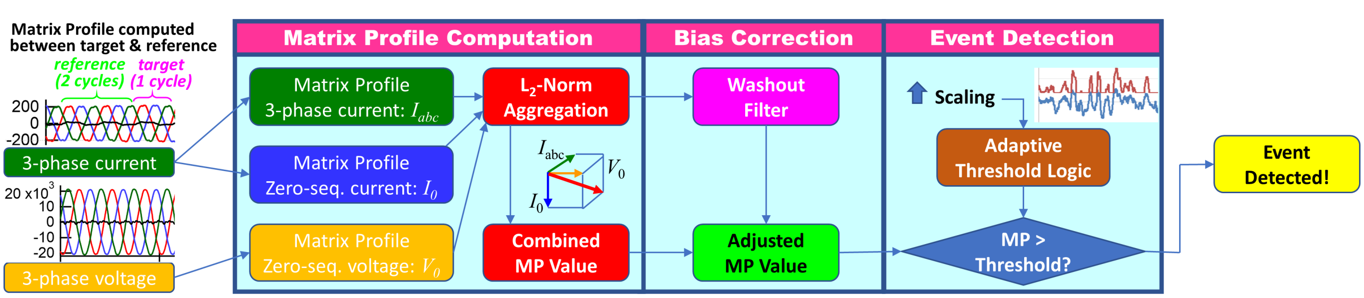

Fig. 1. A schematic of the proposed lightweight Matrix Profile–based framework for real-time abnormal event detection using PoW measurements.

overlapping subsequences of fixed length m corresponding to one cycle of the waveform at sampling rate f_s.

The i-th target subsequence is defined as (1). Each target subsequence $\mathbf{X}_i$ is compared against a reference set $\mathcal{R} = \{\mathbf{R}_{i-m-n+1}, \ldots, \mathbf{R}_{i-m}\}$ consisting of n subsequences extracted from historical measurements representing normal operating conditions (see (2) for subsequence $\mathbf{R}_{i-m}$).

$$\mathbf{X}_i = [\mathbf{x}(i-m+1), \mathbf{x}(i-m+2), \ldots, \mathbf{x}(i)] \in \mathbb{R}^{m\times D}. \quad (1)$$

$$\mathbf{R}_{i-m} = [\mathbf{x}(i-2m+1), \ldots, \mathbf{x}(i-m)] \in \mathbb{R}^{m\times D}. \quad (2)$$

The reference set includes not only three-phase current signals, but also their zero-sequence voltage and current. To explicitly indicate the sliding window relationship, the reference subsequences are shifted relative to the current subsequence. This ensures each comparison is made with sequences of the same length while avoiding trivial self-matches.

For each channel $d \in \{1, \ldots, \mathcal{D}\}$, the distance between the d-th channel of $\mathbf{X}_i$ and a reference subsequence $\mathbf{R}_j$ is computed using the z-normalized Euclidean distance:

$$\mathrm{dist}\Big(\mathbf{X}_i^{(d)}, \mathbf{R}_j^{(d)}\Big) = \left\| \frac{\mathbf{X}_i^{(d)} - \mu_i^{(d)}}{\sigma_i^{(d)}} - \frac{\mathbf{R}_j^{(d)} - \mu_j^{(d)}}{\sigma_j^{(d)}} \right\|_2, \quad (3)$$

where $\mu^{(d)}$ and $\sigma^{(d)}$ denote the mean and standard deviation of the corresponding subsequence.

The multivariate distance between $\mathbf{X}_i$ and $\mathbf{R}_j$ is obtained by aggregating the distances across all channels:

$$D(\mathbf{X}_i, \mathbf{R}_j) = \sqrt{\sum_{d=1}^{\mathcal{D}} \Big(\mathrm{dist}\Big(\mathbf{X}_i^{(d)}, \mathbf{R}_j^{(d)}\Big)\Big)^2}. \quad (4)$$

The matrix profile value at index i is defined as (5) [14].

$$\mathrm{MP}[i] = \min_{\mathbf{R}_j \in \mathbb{R}} D(\mathbf{X}_i, \mathbf{R}_j). \quad (5)$$

B. Selection of PoW Signals for Anomaly Detection

For real-time streaming anomaly detection, minimizing the number of measurement channels is critical to reduce computational burden and communication overhead at the grid edge. Although most short-circuit faults are unbalanced, balanced events such as induction motor starting and transformer energization also occur in practice. Therefore, three-phase current measurements are required to detect a broad spectrum of power system events. In addition, zero-sequence voltage and current provide complementary information for unbalanced conditions, where only a subset of phases may exhibit pronounced deviations. Three-phase voltage measurements are excluded, as they typically offer limited incremental sensitivity beyond current-based indicators under normal grid operating conditions. Based on these considerations, three-phase current, zero-sequence voltage, and current are selected as inputs to the proposed MP-based event detection framework.

C. Washout Filter-based Bias Correction

Under balanced three-phase conditions, zero-sequence components of voltage and current are near zero. However, load asymmetry or distorted currents can create a persistent bias in the MP, resulting in false positives even in the absence of grid events. To mitigate this bias, a first-order washout filter is applied to the MP values:

$$H(s) = \frac{\tau s}{1 + \tau s}, \quad (6)$$

where τ is the time constant in seconds.

The time constant of 0.1 s is selected to ensure rapid attenuation of steady-state components while preserving transient dynamics associated with system faults, which typically persist for approximately three to five fundamental cycles. Under the baseline model, a fixed detection threshold for filtered MP values can be determined by balancing detection sensitivity against false positive suppression.

D. Dynamic Threshold for MP Values

Although the washout filter significantly reduces false positives, a fixed detection threshold may still be insufficient under varying current distortion levels. In particular, persistently unbalanced currents accompanied by high random noise at steady state can produce large fluctuations in the MP around zero, with intermittent peaks approaching or exceeding the fixed threshold, thereby leading to spurious detections.

To further suppress false positives under such conditions, a dynamic threshold mechanism is introduced. The fundamental concept is to adaptively scale the detection threshold based on recent MP magnitudes, allowing the threshold to accommodate elevated baseline fluctuations while preserving sensitivity to genuine transient events. Specifically, a scaling factor is computed using the mean of the most recent N MP samples, given by

$$\bar{\mathrm{M}}\mathrm{P}[i] = \frac{1}{N} \sum_{n=0}^{N-1} \mathrm{MP}[i-n]. \quad (7)$$

The dynamic detection threshold is then defined as

$$\gamma[i] = \max\big(\gamma_0,\ \gamma_0(1 + \alpha\, \bar{\mathrm{M}}\mathrm{P}[i])\big), \quad (8)$$

where γ_0 denotes the original fixed threshold and α is a scaling constant. The window length N is selected empirically with sample real-world measurement data.

The selection of the MP averaging window entails a fundamental trade-off between responsiveness and stability. An excessively long window causes the detection threshold to adapt slowly to changes in the baseline MP level. When sustained oscillations occur, the threshold remains close to its long-term average, allowing repeated upward fluctuations to exceed it and thereby increasing the false positive rate. Conversely, an overly short window enables the threshold to track MP variations too aggressively. In this case, the threshold rises nearly in tandem with the MP signal, reducing the detection margin and potentially suppressing true events, which increases the false negative rate. Constraining the dynamic threshold to remain no

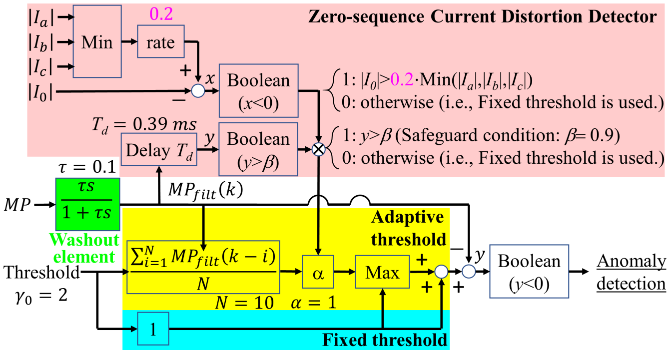

Fig. 2. Matrix profile-based anomaly detection diagram.

lower than γ_0 prevents excessive sensitivity degradation under nominal operating conditions. To further enhance detection robustness, the dynamic threshold mechanism is activated only under severely distorted current conditions, such conditions are defined as cases in which the zero-sequence current magnitude constitutes significant fraction of the three-phase current magnitude. From a safeguard perspective, activation occurs only when the filtered MP values with a short delay T_d exhibits a pronounced bias, thereby preventing unnecessary threshold adaptation under normal operating conditions.

It should be noted that the adaptive threshold does not introduce additional detection latency. Because the threshold increases gradually based on the moving average of past MP values, abrupt MP rises caused by actual events still exceed the threshold promptly. In contrast, instantaneous threshold adaptation could completely mask genuine events. Thus, the conditional time-varying threshold substantially reduces false positives, at the cost of a slight reduction in true positives. The entire anomaly detection flow is illustrated in Fig. 2.

IV. Case Study

The proposed MP-based power grid event detection method is validated using actual PoW data across the United States. This section details the validation study, highlighting the real-time detection performance and required hardware specification, specifically the RAM usage.

A. Data Source and Measurement Characteristics

Publicly available PoW data are provided by the Event Signature Library [16], which contains more than 100 recorded events with sampling rates, f_s, ranging from 7,680 Hz to 20,000 Hz, 15,360 Hz being the most common. Because high-rate measurements can be readily down-sampled without loss of critical event information, the lowest rate (7,680 Hz) is selected as a conservative and practically deployable design target for the proposed event detection framework. The root causes of the considered events include conventional short-circuit faults as well as various switching operations, such as capacitor bank connection and disconnection. Electric utility-provided event timings and types are all included in the library. The affected power equipment spans a broad range of system components, as illustrated in Fig. 3. The target time series length m is set at 130. The MP averaging window length,

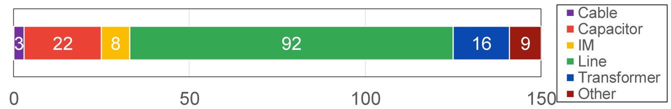

Fig. 3. Distribution of power grid events by power equipment type.

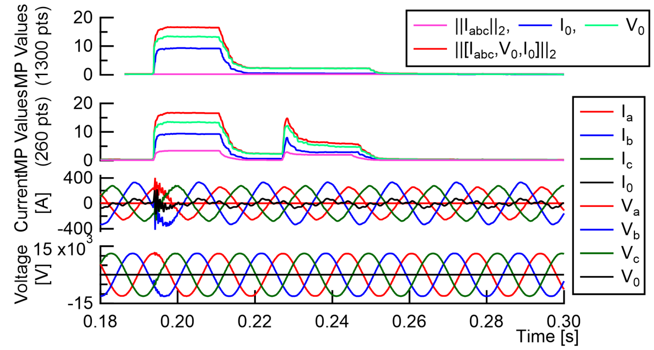

Fig. 4. MP values (short-circuit event with reference time-series length of 260 and 1300 points/samples)

which is the most sensitive hyperparameter, is set to $N = 10$. The parameter γ_0 is empirically tuned to 2 using PoW data, while α is fixed at 1. Because short-circuit faults can be reliably detected by existing protection and monitoring devices as well as by the proposed method, this paper focuses mainly on the detection capability for switching events.

B. Event Detection Performance

1) Impact of Reference Time-series Length on Detection Performance: The length of the reference time-series window is a key factor in achieving real-time event detection using PoW measurements. A shorter window reduces computational and memory requirements, which is critical for grid-edge deployment; however, an overly short window may fail to capture steady-state behavior and degrade detection reliability. Figure 4 compares MP values obtained using reference windows of 260 and 1300 samples and demonstrates that the shorter window achieves the same anomaly onset detection latency as the longer window. However, a shorter window may yield distinct feature patterns for subsequent events, which can affect event discrimination. Nevertheless, from a grid-monitoring perspective, the primary objective is the timely and reliable detection of the first abnormal event rather than the precise characterization of all subsequent disturbances. Therefore, considering the trade-off between computational efficiency and detection performance, a reference window length of 260 samples is selected, as it enables fast and reliable anomaly detection under tight resource constraints.

2) Comparative Detection Performance Across Measurement Signals: Representative detection results are shown in Figs. 5, 6, and 7. Figure 5 shows that the motor start event is most clearly detected using three-phase current, whereas Fig. 6 indicates that transformer energization is most effectively captured by zero-sequence current. Similarly, Fig. 7 demonstrates that the capacitor switching event is most sensitively detected using zero-sequence components. These examples highlight that detection performance depends strongly on the

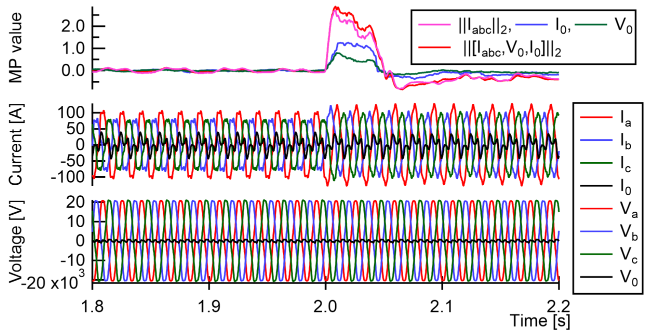

Fig. 5. MP value for motor start (260-sample reference window).

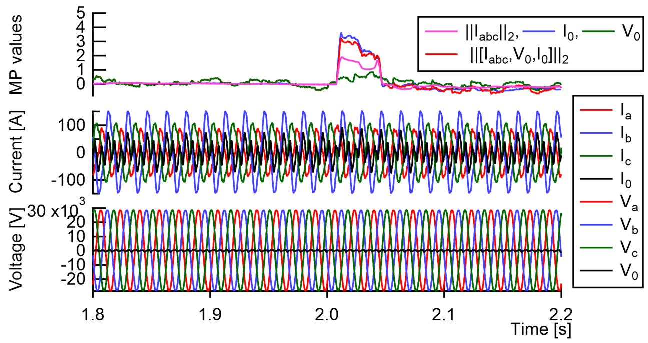

Fig. 6. MP value for transformer inrush (260-sample reference window).

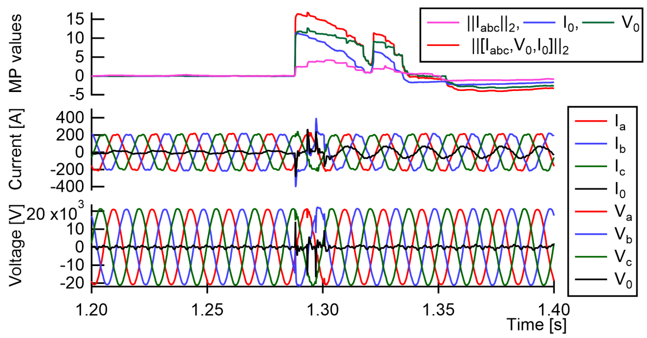

Fig. 7. MP value for capacitor switch (260-sample reference window).

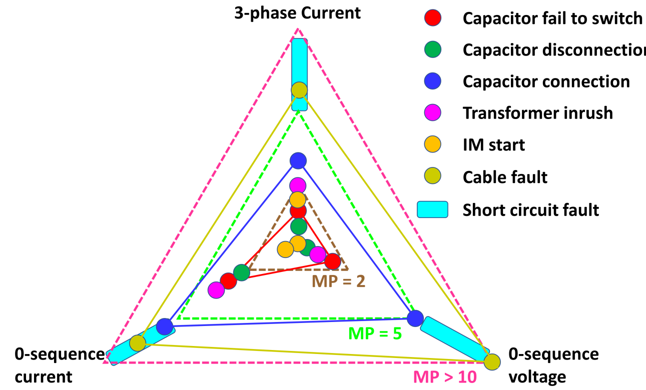

Fig. 8. Anomaly detection capability of various electrical signals

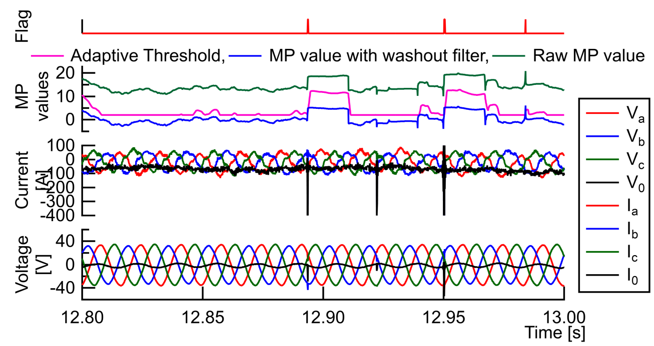

Fig. 9. Successful short-circuit detection (260-sample reference window).

measured quantity: three-phase current, zero-sequence current, and zero-sequence voltage are each sensitive to different types of events, and no single quantity consistently detects all events. As illustrated in Fig. 8, combining the matrix profile indicators from these three signals yields reliable detection across all evaluated event types, validating the selected electrical signal set for the proposed framework.

3) Impact of Washout Filter on Event Detection: The effect of the washout filter is illustrated in Fig. 9. For largely balanced three-phase currents, the filter has negligible impact on MP values. In contrast, under distorted or unbalanced currents, the unfiltered MP exhibits a persistent rise, which can lead to false detections when a fixed threshold is applied. With the washout filter enabled, this steady-state bias is effectively suppressed, and the MP is re-centered near zero during normal operation while preserving sensitivity to genuine transients. Quantitatively, applying the washout filter reduces the number of false positives from 15 to 10 over the evaluation dataset, confirming its effectiveness in mitigating bias-induced spurious detections. Nevertheless, residual fluctuations under severely distorted steady-state conditions can still trigger false positives, which motivates the adaptive thresholding strategy.

4) Impact of Adaptive Threshold on Event Detection: Examples of the adaptive threshold are also shown in Fig. 9. The threshold is constructed using a 10-sample moving average, which suppresses low-frequency variations in the MP and prevents slow baseline fluctuations from triggering false alarms. The activation condition consists of 20% zero-sequence current magnitude of three-phrase current magnitudes with the safeguard value, β of 0.9 and T_d of 0.39 ms. At the onset of a grid event, the MP typically exhibits a step-like increase that is not tracked by the moving average, allowing the event to be detected reliably (see Fig. 9).

Quantitatively, introducing the adaptive threshold further reduces the number of false positives from 10 to 0. However, this improvement comes at the cost of increased missed detections: the number of false negatives increases by 5. Despite this trade-off, combining the washout filter with the adaptive threshold achieves an F1 score of 95.3%, with a recall of 90.7% and a precision of 100%. From an event detection standpoint, minimizing false positives is particularly important, as spurious alarms can trigger unnecessary monitoring actions and reduce operator confidence in the detection system.

C. FFT Acceleration and Real-Time Implementation

To support streaming matrix profile updates, fixed-size FFT in the west (FFTW) plans are created once during initialization (two forward and one inverse transforms) with a transform length of $2m$. Because the transform size remains constant,

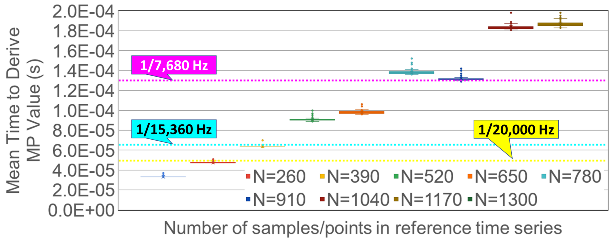

Fig. 10. Average time to derive MP value in seconds.

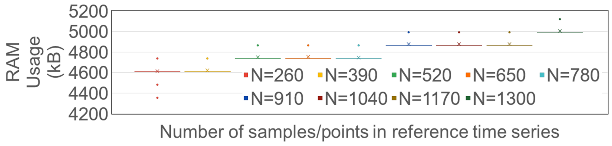

Fig. 11. Maximum RAM usage.

these plans are reused throughout execution, eliminating FFT planning overhead during runtime. As shown in Fig. 10, the average processing latency for a 260-sample reference window is approximately 50 μs, which is well below the sampling interval and confirms real-time performance, significantly faster than typical event-classification inference times (12.3 ms) [17].

D. CPU Memory usage

The resident set size (RSS) is also monitored to quantify the physical memory footprint of the proposed algorithm during execution. As shown in Fig. 11, the RSS remains constant across the entire streaming operation, indicating that all required memory—including FFTW working buffers, plans, and auxiliary arrays—is allocated during initialization and no further dynamic memory allocation occurs online. When varying the length of the reference time series, the RSS exhibits a step-wise increase rather than a continuous growth pattern. Specifically, similar RSS values are reported for multiple consecutive reference window lengths, followed by a discrete increase once a certain threshold is exceeded. Importantly, for the selected 260-sample reference window, total memory usage remains below 5 MB, confirming that the proposed method is highly memory-efficient and well-suited for grid-edge deployment.

V. Conclusion

This paper presented a lightweight matrix profile–based framework for real-time abnormal event detection using PoW measurements, addressing the practical constraints of grid-edge deployment under high sampling rates. By selecting the most informative electrical signal quantities from historical PoW data and labeled events, and by incorporating washout filtering together with an adaptive time-varying thresholding scheme, the proposed approach improves detection accuracy, particularly under severely distorted three-phase current conditions. The method was validated on more than one hundred real-world PoW records, demonstrating reliable real-time detection performance at a sampling rate of 7,680 Hz while requiring only 5 MB of memory. These results indicate that the proposed framework effectively balances detection accuracy, computational efficiency, and memory usage, making it suitable for deployment on resource-constrained edge devices in modern power grids.

This work demonstrates the feasibility of high-resolution, data-driven abnormal event detection at the grid edge using PoW measurements under strict computational and memory constraints. The proposed framework focuses on timely event indication rather than event classification. Although the adaptive threshold enhances robustness under unbalanced conditions, it may reduce sensitivity to slowly evolving events. Future work will address this trade-off, extend the framework to event classification, and further improve detection performance across diverse event dynamics.

References

[1] PNNL and NIST Team, "PMU data quality: A framework for the attributes of PMU data quality and a methodology for examining data quality impacts to synchrophasor applications," NASPI, NASPI-2017-TR-002/ PNNL-26313, Mar. 2017.

[2] R. R. Hossain, K. Mahapatra, and J. P. Ogle, "Model agnostic Bayesian framework for online anomaly/event detection in PMU data," in *2023 IEEE PES GM*, 2023, pp. 1–5.

[3] Y. Liu, L. Yang, A. Ghasemkhani, H. Livani, V. A. Centeno, P.-Y. Chen, and J. Zhang, "Robust event classification using imperfect real-world PMU data," *IEEE Internet Things J.*, vol. 10, no. 9, pp. 7429–7438, 2023.

[4] F. Han, P. M. Ashton, M. Li, I. Pisica, G. Taylor, B. R. Rawn, and Y. Ding, "A data driven approach to robust event detection in smart grids based on random matrix theory and Kalman filtering," *Energies*, vol. 14, no. 8, p. 2166, 2021.

[5] R. Pourramezan, H. Karimi, and J. Mahseredjian, "Synchrophasor network-based detection and classification of power system events: A singular value decomposition approach," *Electr. Power Syst. Res.*, vol. 223, p. 109645, 2023.

[6] J. Shi, B. Foggo, X. Kong, Y. Cheng, N. Yu, and K. Yamashita, "Online event detection in synchrophasor data with graph signal processing," in *Proc. IEEE Int. Conf. Commun., Control Comput. Technol. Smart Grids (SmartGridComm)*, 2020, pp. 1–7.

[7] X. Kong, B. Foggo, K. Yamashita, and N. Yu, "Online voltage event detection using synchrophasor data with structured sparsity-inducing norms," *IEEE Trans. Power Syst.*, vol. 37, no. 5, pp. 3506–3515, 2022.

[8] T. Yin, S. Wulff, J. W. Pierre, and B. Amidan, "Event detection and classification using machine learning applied to PMU data for the Western US power system," in *2024 Int. Conf. Smart Grid Synchronized Meas. Anal.*, 2024, pp. 1–6.

[9] Y. Cheng, N. Yu, B. Foggo, and K. Yamashita, "Online power system event detection via bidirectional generative adversarial networks," *IEEE Trans. Power Syst.*, vol. 37, no. 6, pp. 4807–4818, 2022.

[10] A. Aligholian, A. Shahsavari, E. Stewart, E. Cortez, and H. Mohsenian-Rad, "Unsupervised event detection, clustering, and use case exposition in micro-PMU measurements," *IEEE Trans. Smart Grid*, vol. 12, no. 4, pp. 3624–3636, Jul. 2021.

[11] Y. Liu, L. Yang, and J. Zhang, "Automatic labeling of real-world PMU data: A weakly supervised learning approach," *Electronics*, vol. 14, no. 23, p. 4703, 2025.

[12] J. Shi, B. Foggo, and N. Yu, "Power system event identification based on deep neural network with information loading," *IEEE Trans. Power Syst.*, vol. 36, no. 6, pp. 5622–5632, 2021.

[13] L. Tong, X. Wang, and Q. Zhao, "Grid monitoring with synchro-waveform and AI foundation model technologies," *Energy Syst.*, 2025.

[14] The UCR Matrix Profile Page, "The UCR matrix profile page," https://www.cs.ucr.edu/ eamonn/MatrixProfile.html, 2019.

[15] M. Frigo and S. G. Johnson, "The design and implementation of FFTW3," *Proc. of the IEEE*, vol. 93, no. 2, pp. 216–231, 2005.

[16] U.S. Department of Energy, ORNL, "Grid event signature library," https://gesl.ornl.gov/login, 2024, accessed: 2026-02-05.

[17] M. Mozaffari, K. Doshi, and Y. Yilmaz, "Real-time detection and classification of power quality disturbances," *Sensors*, vol. 22, no. 20, 2022.